NAIC-ID(RS)T-0385-94

NATIONAL AIR INTELLIGENCE CENTER

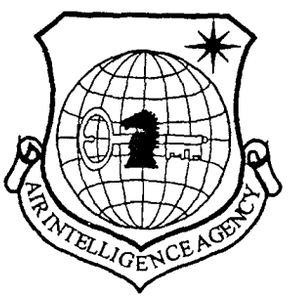

ROOM-TEMPERATURE PHOTOCURRENT SPECTROSCOPY OF GaAs/GaAlAs MULTIPLE QUANTUM WELLS

by

Duan Hailong, Wang Qiuning, et al.

I

NAIC- ID(RS)T-0385-94

HUMAN TRANSLATION

NAIC-ID(RS)T-0385-94 15 November 1994

MICROFICHE NR: 94C000483L

ROOM-TEMPERATURE PHOTOCURRENT SPECTROSCOPY OF GaAs/GaAlAs MULTIPLE QUANTUM WELLS

By: Duan Hailong, Wang Qiuning, et al.

English pages: 12

Source: Bandaoti Xuebao, Vol. 12, Nr. 7, July 1991, pp. 399-404

Country of origin: China
Translated by: Leo Kanner Associates
F33657-88-D-2188
Quality Control: Nancy L. Burns
Requester: NAIC/TATE/Capt Joe Romero

GRAPHICS DISCLAIMER

All figures, graphics, tables, equations, etc. merged into this translation were extracted from the best quality copy available.

ROOM-TEMPERATURE PHOTOCURRENT SPECTROSCOPY OF GaAs/GaAlAs MULTIPLE QUANTUM WELLS

DUAN HAILONG, WANG QIUNING, WU RONGHAN, ZENG YIPING and KONG MEIYING

Institute of Semiconductors, Academia Sinica, Beijing 10083)

By means of room temperature photocurrent spectroscopy, we have studied the effect of electric fields on exciton absorption in GaAs/GaAlAs multiple quantum wells (MQW) and discuss in this paper the effect of an electric field on the photocurrent spectra for some kinds of MWQ structures. The material requirement for related optoelectric devices MQW is also discussed.

I: INTRODUCTION:

In the past several years there has been enthusiasm over the technology of opitaxy of films of different materials. it has become possible to use superlattice quantum trap materials to construct practical devices. In quantum trap materials, the electrons and space are restricted by potential barriers, increasing the ability to trap two dimensional free electrons, allowing the excitons to exist at room temperatures and in strong electrical fields ($\sim 10^5$v/cm). When there is an applied electrical field perpendicular to the quantum trap, because of the quantum controlling stark effect (QCSE)[1], The exciton absorption peak moves in the direction of a long wave, and the exciton absorption intensity is also corresponding reduced. Using the quantum controlling stark effect, it is possible to manufacture a series of brand new optical devices. In this article, through the use of the principle of room temperature photocurrent spectra, we present a study of the effects of an electrical field on the exciton absorption behavoir of multiple layered quangum well (MQW) structures. The electrical field effect on the absorption spectra

of different MQW materials is studdied as well as the material requirements of photoelectronic devices using the quantum controlled stark effect.

II: SAMPLES AND TESTING EQUIPMENT]

The sample materials we used were molecular beam extension prepared MQW materials which possessed typical pin structure. The base was n^+ GaAs with sequential extension layers of n^+ GaAs burrer, n^+ GaAlAs (~2μm), non doped grown (i model) GaAs/AlGaAs multiple quantum trap layers, p model GaAlAs layer (~1μm) P^+ model super thin GaAs top layer, the extension chip had its base thinned, the n face was an AuGeNi electrode, the P face was a CR-AU electrode, and a light aperature was etched into the P face. Then the alloys formed ohm contact. The finished samples were cleaned, scintered, and then soldered with electrodes and installed in seat, forming a device for the testing of photocurrent.

Fig 1: Block Diagram of Photocurrent Spectra Test Equipment

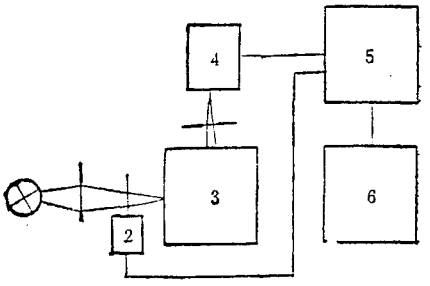

1. Halogen lamp. 2. Chopper. 3. Monochromator. 4. Device being tested. 5. Phase locked amplification. 6. x-y recorder.

Illustration One is a block diagram of photocurrent spectra testing equipment. We used an ordinary halogen lamp as a white light source. It was focussed through a lens onto the monochromator producing monochromtic light. This was directed onto

the device being tested to produce a photocurrent, and through the use of resistors this was sampled and converted to a voltage signal which was sent to the locked phase amplifier and amplified and recorded by the x-y recorder. During the testing, the slits for the light into and out of the monochromator were adjusted to resolution of about 10 angstroms. During testing, the photovoltage was bround the level of 10^{-9}A.

The numbers assigned to the samples tested and their strutural parameters were as shown in Table One.

TABLE 1: Sample Parameters

(1) 编 号	(2) 阱宽(Å)	(3) 势垒宽度(Å)及 Al 含量		(4) 周 期 数
1#	130	60	$x = 1$	100
2#	110	100	$x = 0.3$	40
3#	100	100	$x = 0.2$	10

1. Sample number. 2. Well width (Å). 3. Potential barrier width (Å) and Al content. 4. Cycles.

III: RESULTS AND PRELIMINARY ANALYSIS OF PHOTOCURRENT TESTING

Illustration Two shows the photocurrent of sample number one.

Sample number one was GaAs/AlAs. Its potential barrier thickness was 60 angstroms. Its potential barrier and trap zones bandgap varied in width as much as 1.6 Ev. Because there was a fairly high potential barrier it allowed the quantum trap to be able to have a failry large number of sub energy levels, and in the photocurrent spectrum of different bias voltages, we were able to see a number of forbidden transitions occur. This will be discussed in detail later in this paper.

Because of the weak coupling between the traps, we were able to use limited depth trap models to perform preliminary analysis of

changes in the sub energy levels of the square quantum traps as the applied electrical field was changed and to ignore the effects of the potential barrier zone electroical field on the compoutation of the energy levels of low sub energy bands. The parameters used in the computatins were trap width l_ω= 130 angstroms, electron effective mass $m_e^*=0.0667m_0$, heavy hole effective mass $m_{hh}^*=0.34m_0$, , light hole effective mass $m_{lh}^*=0.094m_0$, , lead band discontinuity ΔV_c = 1.09eV , valence band discontinuity ΔV_v = 0.5 eV , forbidden zone width $E_g(GaAs) = 1.424$ eV, $E_g(AlAs) = 3.018$ eV.

Fig. 2: Room Temperature Photocurrent Spectra of Sample One at Different Electric Fields (10^4V/CM).

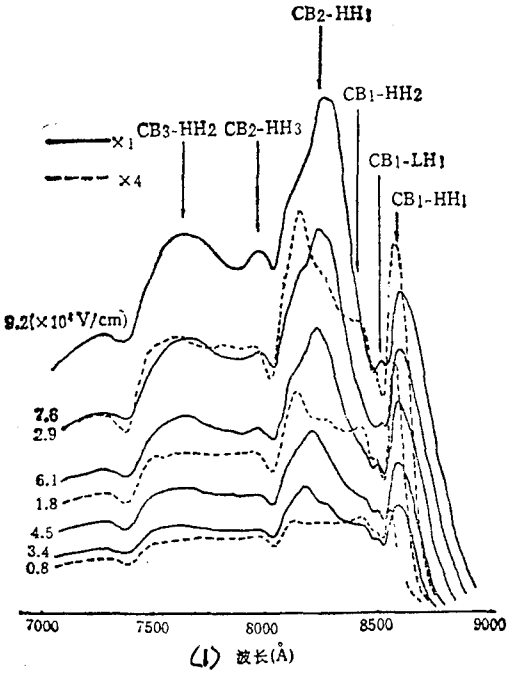

SAMPLE PARAMETERS: GaAs/AlAs, MQW 130Å/60Å, 100 cycle.
Illustation shows exciton transition between sub energy levels.

1. Wave length Å.

Fig. 3: Results of Computations of Sub Energy Level Transition Energy wtih Changes in Electrical Field

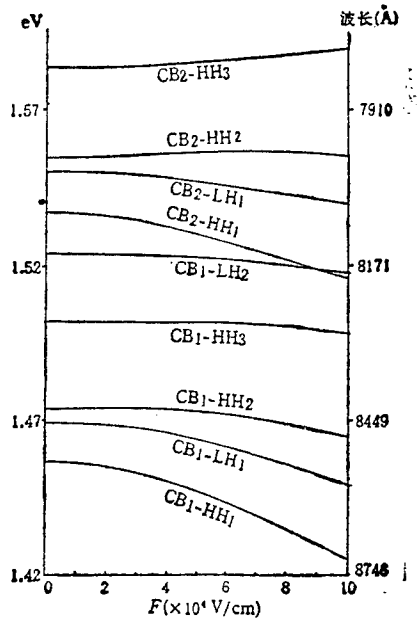

TRAP WIDTH l_ω = 130 Å.

To calculate the perpendicular seperation sub energy levels created by the quantum traps, we solved the following Schrodinger equations:

$$\begin{cases} \left(-\frac{\hbar^2}{2m^*}\frac{d^2}{dz^2}+\Delta V\right)\phi = E\phi & z<0 \quad (\text{势垒区}) \\ \left(-\frac{\hbar^2}{2m^*}\frac{d^2}{dz^2}+eFz\right)\phi = E\phi & 0\leqslant z\leqslant l_w \quad (\text{阱区}) \\ \left(-\frac{\hbar^2}{2m^*}\frac{d^2}{dz^2}+eF\cdot l_w+\Delta V\right)\phi = E\phi & l_w<z \quad (\text{势垒区}) \end{cases} \tag{1}$$

Herein, m* is the effective mass, F is the strength of the electrical field, ΔV is the energy band value of discontinuity, for electrons, $\Delta V = \Delta V_{c9}$ and for light and heavy holes, $\Delta V = \Delta V\gamma$. We solved the equations with the numerical method.

Illustration Three shows the changes in the energy level differentials of the various energy fields as the electrical field is changed. (CB1 indicates the electron sub energy level where n=1, HH1 indicates the heavy hole sub energy level whiere n=1 and LH1 indicates the light hole sub energy level where n=1). We can

see from this that the energy level differential (ie transition energy) between a number of low sub energy bands is reduced with an applied electrical field, taht is the sub energy band absorption boundary shifts in the direction of the long wave. Changes in the exciton binding energy was not calculated here. Considering this factor, the changes in the transition energy of the individual sub bands with the electrical field may vary at the most a few meV from what is shown in Illustration Three[2]. Using CB1-HH1 as an example, the exciton binding energy will decrease by several meV with the addition of a electrical field, but its energy level shift will be greater than 30 meV when the electrical fleld is 10^3v/cm. Therefore, the overall effect is that the n=1 exciton absorption peak will shift toward the direction of the long wave (ie toward low energy) (the Quantum controlled Stark Effect).

The exciton absorption factor $\alpha(F)$ satisfies the following equation:

$$\alpha(F) \propto \frac{\left| \int_{-\infty}^{+\infty} \phi_e(z) \phi_h(z) dz \right|^2}{\alpha_B^3 l_\omega} \qquad (2)$$

Herein, F is the strength of the electric field, α_B is the exciton Bohr radius, l_ω is the trap width, $\phi_e(z)$、$\phi_h(z)$ are the electron and hole envelope wave factors respectively. When an applied electrical field does not exist, because of the criss crossing of the different wave factors between the sub bands, the transition only occurs between $\Delta N=0$ sub energy levels. When the applied electrical field is added, the dipersion of the wave factors of the electrons and holes shifts toward either end, and the Δn-0 wave factor overlapping integration is reduced, $\Delta n=0$ transition probability is reduced and the overlapping integration between the $\Delta n \neq 0$ lead band and balence band begnis to increase, leading to the occurance of an $\Delta n \neq$ transition (ie forbidden transitions occur). Under a certain electrical field strength, $\Delta n=\pm 1$ transitions exceed the $\Delta n=0$ transitions. The electrical field strength necessary for this change to occur depends on the trap width. The wider the trap, the more the distribution of the envelope wave factors of the

electrons and hole wave forms are influenced by the electrical field, so a lower intensity electric field is required for the the change to occur. For a 150 Å trap, the change occurs at moderate electrical field intensity ~3-4 X 10^4v/cm[4]. Af for using barrier levels of different X values, with higher X values, or the high potential barrier, has a stronger limitation of the (current) carrier in the trap, and its electrical field effects are somewhat weaker than those on low potential barriers. However, the electrical field effect is far less sensitive to changes in the height of the potential barrier than to trap width.

The potential barrier material of sample one was AlAs. It possesses fairly potential barrier qualities. This sample allowed for more sub energy levels to exist in the trap, and with an applied electrical field we saw exciton transition between a number of sub energy levels. Illustration Two shows some of the primary transitions.

It is worth explaining that there was a rapid increase in the photocurrent in the photocurrent spectra when the voltage of the applied electrical field was increased, with a stepped decrease in the directin of the short waves. Also, there were photocurrent valleys near 7400Å, 8000Å and 8500Å. We believe that this is primarily caused by the following factors. Sample number one had a fairly thick quantum trap (1.9μm), and its base residual was P model, only that portion of the quantum trap mear the base was depleted. When the light was directed from P, it must first pass through zone MQW which had no electrical field for a portion to be absorbed before it reached the depletion MQW region. Only depletion region absorption contributes to photocurrent (here we ignore the diffusion current of the space charge region). This creates the stepped decrease in the photocurrent spectrum in the direction of the short waves. Photocurrent valleys also occured at the locations corresponding to sub band exciton absorption peaks (these characteristics were most obvious in the low bias voltage

photocurrent spectra). As the applied voltage is increased, the depletion zone expanded, and the photocurrent increased. In addition, the complex transport process in the quantum trap regions can also have an effect on the form of the photocurrent spectra, but just how much of an effect is not yet clear. The lack of uniformity of the electric field distribution and non depleted MQW domain absorbtion has an effect on the shape of the photocurrent spectra. This makes it difficult to conduct quantative comparative analysis on the transition behavoir of the individual transition energy levels, and even makes it difficult to come up with an accurate actual quantum trap zone electric field value for each applied voltage. Illustration Two provides rough estimates of electric field strength.

Fig. 4. Room tempertature Photocurrent Spectra of Sample Two at Different Electric Fields (10^4V/cm)

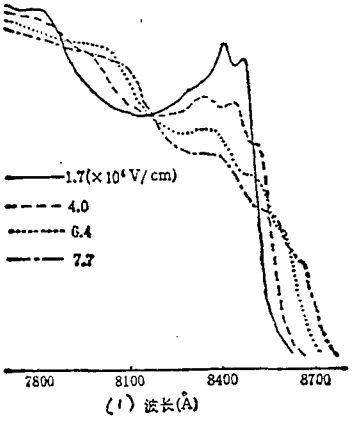

SAMPLE PARAMETERS: $GaAs/Ga_{0.7}Al_{0.3}As$. MQW 110Å/100Å, 40 cycles.
1. Wave length Å.

Illustration Four shows the result of the photocurrent spectra experiments using Sample Number Two. We can see from this illustration that at the short wave portion there is no major change in the photocurrent values as the voltage is increased. It may be takenm that there is little change in the absorption index as the electric field undergoes changes. Photocurrent saturation indicates that under the effect of a built-in field (ie when the

electric field intensity is 1.7 X 10^4V/cm) the quantum trap zone is completely depleted (quantum trap zone total thickness was about 0.84μm), so changes in photocurrent near the exciton peak wavelength is primarily caused by changes in the absorbtion coeficient, with the quantum controlled stark effect playing the rimary role. From the photocurrent spectra we can see that as the applied voltage is increased, the exciton absorption peak shifts toward the direction of longer waves, and furthermore, the light and havy hole absorption peaks are not so high (this indicates that at this time the electric field is not sufficient to cause the excitons to be completely dissociated). When the applied voltage is primarily directed at the MQW domain, the field intensity of the MQW domain is equal to the built-in potential plus the applied voltage minus the thickness of the MQW domain. As the strength of applied electric field is increased, we also see forbidden transition exciton peaks CB1-HH2 and CB2-HH1.

Fig 5: Room temperature Photocurrent Spectra of Sample Three at Different Voltages (10^4V/cm)

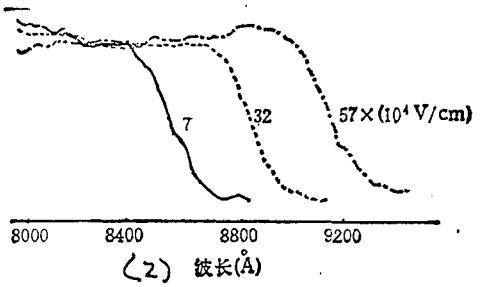

SAMPLE PARAMETERS: GaAs/$Ga_{0.8}Al_{0.3}As$. MQW 100Å/100Å to cycles.

Illustration Five shows the results of photocurrent spectra experiements using sample three. When the applied voltage was 0V, no clear exciton peak could be seen. As the applied voltage was increased, the photocurrent value did not chnge, but only shifted in the direction of longer waves. This indicates that the potential barriers are very low and the total thickness of the quantum well zone is very small (-0.2μm). Furthermore, the base

residual is very concentrated, leading to a very strong built-in field, causing exciton disocciation, and the absorption boundary red shift was determined by low sub band energy level which changed with the electric field.

IV: CONCLUSIONS

In the article above, we have discussed the relationships between three typical room temperature photocurrent spectra and bias voltage (electric field) and the wave length of incomming light. In the first sample GaAs/AlAs, the space charge region was smaller thyan the Multiple Quangtum Well zone. According to structural design and experimental analysis, within the range of the applied voltage, an electric field of moderate intensity dows not cause exciton dissociation. Furthermore, the potential barrier is very high, causing the various transition characteritics to be clearly detectable. In sample number two, the space charge region was always larger than the MQW zone at moderate electric fields. The well zone field clearly followed changes in the applied bias. In addition the electric field was still not sufficient to cause exciton dissociation. Therefore the sample displayed obvious red shifts and changes in absorption intensity (QCSE). As for sample number three, the built-in field already basically caused exciton dissociation. The space charge region penetrated the fairly thin multiple quantum wells. Therefore, under the effect of an applied electric field, it exhibited a very large red shift energy levels. Based on experimental results, the red shif of the absorption boundary was about 500Å at a voltage of 10V. Therefore, through photocurrent spectra testing, we are able to learn information about the growth quality of material and the width of the quantum wells based on the two dimensional free exciton peak aborption bracketing. From how the photocurrent amplitude follows changes in the applied voltage we obtain information about the concentration of the base of the quantrum well zone. Under the effect of an applied voltage, changes in forbidden and non forbidden transitions

contain even more obtuse physics. However, what is of practical significance for current developments in photoelectric devices is the understanding of the effects of of electric fields on quantum well energy levels and two dimensional free excitons through photocurrent spectra, the effects of the quantum controlling stark effect (QCSE), selecting different materials for the manufacture of optical devices based on electric field effects, such as the free electron optical device (SEED)[5] which must, under the effect of an electric field and with minimum quantization of energy levels, have strong changes in red shifts and probability of transition. Sample number two meets these requirements. Using this material, we have already manufactured self-inductance optic bistable devices. Sample number three has a marked band boundary shift, and has a very large elecric field modulation near the absorption boundary, in the absorption index and refraction index. Therefore, it is appropriate for the manufacture of electro-optical modulators (phase and intensity modulation)[7]. Control of base residue of this sample is extremely important. It can cause uneven distribution of the multiple quanmum well electric field toward the Z direction and different locations of well energy levels, leading to a gradient reduction in the absorption electric field effect. In addition, when the residue is highly concentrated, a high voltage is required to cause the MQW zone to be totally depleted. Thus, in the process of increasing the voltage, the depletion zone expands in the MQW zone, causing the absorbtion effect zone to increase (this refers to absorption contributing to photocurrent), and when the depletion zone expansion effet is great it can mask the quantum controlled stark effect, resulting in the material being unuseable for the manufacture of optical devices.

In addition, in applications in practical devices, the width of the potential wells and the potential barriers should be considered. For the usual square potential wells, the effect where the n=1 sub band exciton absorption changes with the external electric field (QCSE) varies in an extremely obvious manner as the

width of the potential well changes. When the well is wide, the exciton peak varies markedly with the applied electric field. However, at the same time causing a weakening of the the electron-holes corridor effect, resulting in exciton absorption beak flattening out. When the wells are narrow, the opposite is true. The exciton absorption peaks are sharp, but they vary little as the electric field changes. The effect of the width of the potential barriers has less of an effect than the width of the wells. Because the devices operate using the quantum well portions, potential barriers that are too wide may cause the proportionate operational portion to be smaller, and when the potential barrier is too narrow, it causes an increased probatility of tunnels between the individual wells, decreasing the probability of an electron and hole existing in a well at the same time, widening and lowering the exciton peak (super lattices with very narow potential barriers are a different matter, and are not addressed here). Therefore, choosing the proper width of the quantum wells and potential barriers is very importance in practical applications.

The authors express their appreciation to comrade Luo Liping of the technique line of the Haite Company of this institute and other comrades for their assistance in this work. We express out gratitude to all the comrades of the Bistability Group and the Molecular Beam Extension Group for their assistance and support in this work. We express our appreciation to comrade Jiang Desheng for his assistance and support of this work.

BIBLIOGRAPHY

DISTRIBUTION LIST

DISTRIBUTION DIRECT TO RECIPIENT

ORGANIZATION	MICROFICHE
B085 DIA/RTS-2FI	1
C509 BALLOC509 BALLISTIC RES LAB	1
C510 R&T LABS/AVEADCOM	1
C513 ARRADCOM	1
C535 AVRADCOM/TSARCOM	1
C539 TRASANA	1
Q592 FSTC	4
Q619 MSIC REDSTONE	1
Q008 NTIC	1
Q043 AFMIC-IS	1
E051 HQ USAF/INET	1
E404 AEDC/DOF	1
E408 AFWL	1
E410 AFDTC/IN	1
E429 SD/IND	1
P005 DOE/ISA/DDI	1
P050 CIA/OCR/ADD/SD	2
1051 AFIT/LDE	1
PO90 NSA/CDB	1
2206 FSL	1

Microfiche Nbr: FTD94C000483L
NAIC-ID(RS)T-0385-94